Chemical Science

EDGE ARTICLE

View Article Online
View Journal | View Issue

Cite this: *Chem. Sci.*, 2016, **7**, 5867

Emission color tuning and white-light generation based on photochromic control of energy transfer reactions in polymer micelles†

Magnus Bälter,[a] Shiming Li,[a] Masakazu Morimoto,[b] Sicheng Tang,[c] Jordi Hernando,[d] Gonzalo Guirado,[d] Masahiro Irie,[b] Françisco M. Raymo[c] and Joakim Andréasson*[a]

Received 12th April 2016
Accepted 23rd May 2016

DOI: 10.1039/c6sc01623e

www.rsc.org/chemicalscience

We encapsulate a fluorescent donor molecule and a photochromic acceptor unit (photoswitch) in polymer micelles and show that the color of the emitted fluorescence is continuously changed from blue to yellow upon light-induced isomerization of the acceptor. Interestingly, white-light generation is achieved in between. With the photoswitch in the colorless form, intense blue emission from the donor is observed, while UV-induced isomerization to the colored form induces an energy transfer reaction that quenches the donor emission and sensitizes the yellow emission from the colored photoswitch. The process is reversed by exposure to visible light, triggering isomerization to the colorless form.

Introduction

Molecular systems displaying stimuli-responsive emission color are attracting considerable attention, very often in the quest for white-light emitting materials.[1–3] Emission color tuning and white-light generation (WLG) can be achieved by additive mixing, that is, combining two or more fluorophores in the correct proportion to generate the desired emission color.[4–8] The major downside with this approach is that the addition of material requires physical access, preventing any kind of remote control of the color change. Moreover, the apparent simplicity of additive mixing using fluorescent molecular systems is misleading, as the resulting emission color is typically not the "sum" due to excited state communication between the fluorophores, *e.g.*, energy transfer reactions. Several alternative strategies have therefore been devised and successfully demonstrated lately.[9–28] One such approach is the use of molecular photoswitches (photochromic molecules), most often acting as acceptors in fluorescence resonance energy transfer (FRET) reactions together with a highly fluorescent donor chromophore.[9,10,12,17,18,22,27–30] Due to the intrinsic ability of photoswitches to change color upon isomerization (both in absorption and emission),[31] the FRET process and consequently, the overall emission color can be controlled by photonic means. Common downsides with the systems reported so far are: (i) very low fluorescence quantum yields of the photoswitch, resulting in a dramatically decreased emission intensity when the photoswitch is in the FRET-active fluorescent form; (ii) that the photoswitch cannot be fully converted to the respective isomeric form, limiting the extent of the emission color change; (iii) poor thermal stability of one of the isomeric forms, implying that the system will display emission color changes even in the absence of photoisomerization; and (iv) WLG is very rare.

Here, we present a self-assembled photochromic system where all the above mentioned downsides have been eliminated. We base the approach on 9,10-diphenylanthracene, **DPA**, as the FRET donor and a photochromic diarylethene derivative, **DAE**, as the acceptor photoswitch.

Results and discussion

Scheme 1 shows the structures and the light-induced isomerizations of **DAE**. The open form (**DAEo**) is isomerized to the corresponding closed isomer (**DAEc**) by UV light exposure (365 nm used here, isomerization quantum yield = 0.42).[32] The reverse reaction is triggered by visible light (523 nm used in this study, isomerization yield = 4.0×10^{-4}).[32] Both the UV- and the visible light-induced reactions enrich the sample to 100% of the respective isomeric form. The thermal reaction **DAEc** → **DAEo** is extremely slow (no absorption changes observed after 100 h at 80 °C.)[32]

[a]*Chemistry and Chemical Engineering, Physical Chemistry, Chalmers University of Technology, 41296 Göteborg, Sweden. E-mail: a-son@chalmers.se*

[b]*Department of Chemistry and Research Center for Smart Molecules, Rikkyu University, Nishi-Ikebukuro 3-34-1, Toshima-ku, Tokyo 171-8501, Japan*

[c]*Laboratory for Molecular Photonics, Department of Chemistry, University of Miami, 1301 Memorial Drive, Coral Gables, Florida 33146-0431, USA*

[d]*Departament de Química, Universitat Autònoma de Barcelona, 08193 Cerdanyola del Vallès, Spain*

† Electronic supplementary information (ESI) available: Experimental section; absorption and emission spectra of **DPA** and **DAE** in acetonitrile; steady-state and SPC fluorescence measurements at varying concentrations; redox energies and driving forces for PET reactions; and simulations of the intermolecular donor–acceptor distances in the micelles. See DOI: 10.1039/c6sc01623e

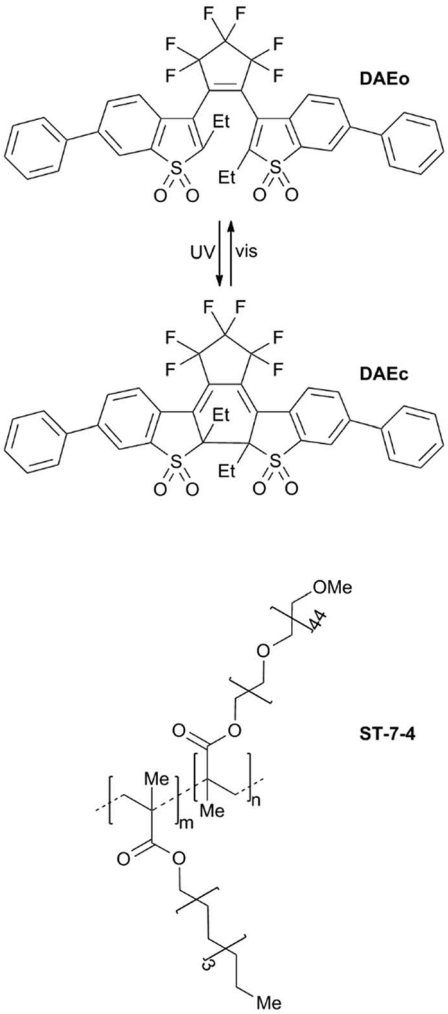

Scheme 1 Isomerization scheme for the DAE derivative used in this study. Also shown is the structure of the ST-7-4 copolymer ($m : n = 6 : 1$).

DPA is a blue emitter with an emission spectrum centered between 400 nm and 450 nm and a fluorescent quantum yield of unity (see Fig. S1 in the ESI† for the spectra of all implicated species in acetonitrile). **DAEo** displays absorption only at wavelengths shorter than 400 nm. This implies that there is virtually no spectral overlap between **DPA** emission and **DAEo** absorption and, hence, that **DAEo** cannot quench the excited state of **DPA** by FRET. On the contrary, there is a substantial overlap between **DPA** emission and the absorption of **DAEc**. The R_0-value for this FRET-pair in acetonitrile was determined to 52 Å, assuming $\kappa^2 = 2/3$. The fluorescence of **DAEc** spans the wavelength region from 500 nm to 700 nm, with an emission maximum at 535 nm. The corresponding quantum yield was determined to be 0.75 in acetonitrile. This value is dramatically higher compared to all other photoswitches from the most common photochromic families, where the typical fluorescence quantum yields are below 0.05.[33]

From the above mentioned spectral features, we anticipated the following scenario upon UV-induced isomerization of **DAEo** to **DAEc** in the presence of **DPA**: with the photoswitch in the **DAEo** isomeric form, unquenched blue emission is observed from the **DPA** donor upon excitation. In the other extreme, UV induced isomerization **DAEo** → **DAEc** is extensive enough for **DAEc** to quench the excited **DPA** with unity efficiency, resulting in exclusively yellow emission from **DAEc**, sensitized in the FRET reaction. However, in all intermediate situations, that is, partial isomerization of **DAEo** to **DAEc**, the overall emission will be a mix between the blue emission from **DPA** and the yellow emission from **DAEc**. Here, the relative contributions depend on the degree of isomerization from **DAEo** to **DAEc** – the larger the isomerized fraction, the more yellow the emission appears.

Both **DPA** and **DAE** are essentially insoluble in water, but are effectively dissolved in the presence of the **ST-7-4** copolymer[34] in aqueous solution by encapsulation into polymer micelles. The structure of the copolymer is displayed in Scheme 1. This particular macromolecular construct incorporates hydrophobic decyl and hydrophilic oligo(ethylene glycol) side chains randomly distributed along a common poly(methacrylate) backbone. Such structural composition promotes the self-assembly of multiple macromolecules into single micelles in aqueous solution. The resulting supramolecular assemblies can encapsulate hydrophobic chromophores in their hydrophobic interior and force them to be in close proximity. As a result, this relatively simple and highly modular noncovalent strategy can be exploited to maintain the complementary components **DPA** and **DAE** at distances compatible with FRET without the need for the tedious synthetic procedures that would, otherwise, be required to constrain them covalently.[35,36] From dynamic light scattering measurements, the average diameter of the micelles was determined to 15 nm. Compared to acetonitrile, both **DPA** and **DAE** retain their photophysical/spectral properties in the micelles, aside from a small overall bathochromic shift (see Fig. 1). Most importantly, the fluorescence quantum yields are not significantly affected, and the photochromic properties of the **DAE** photoswitch are preserved.

Fig. 1 shows the changes in the overall emission spectrum of a water dispersion of the polymer micelles (total micelle concentration *ca.* 1.35 μM) containing **DPA** (total concentration *ca.* 3.5 μM) and **DAE** (total concentration *ca.* 2 μM) upon gradual exposure to 365 nm UV light.[37] It is obvious that the emission intensity of **DAEc** in the micellar "cocktail" does indeed increase with an increasing UV dose, at the expense of the **DPA** emission. It is also seen that the final **DAEc** population cannot quench **DPA** to 100%, as the emission intensity levels off at a non-zero value (see below for a comprehensive evaluation of the quenching efficiencies).

Judging from only the spectral evolution, the perceived color changes of the overall emission is by no means obvious. However, converting each spectrum to a CIE coordinate and mapping the coordinates in the corresponding CIE diagram are a straightforward means to depict the color changes. The result is shown in Fig. 2. Here it is seen that the emission color gradually changes from blue to yellow upon continuous UV-induced isomerization from **DAEo** to **DAEc**. In fact, the emission color of the cocktail virtually spans the entire region between what is observed for **DPA** alone and **DAEc** alone, which

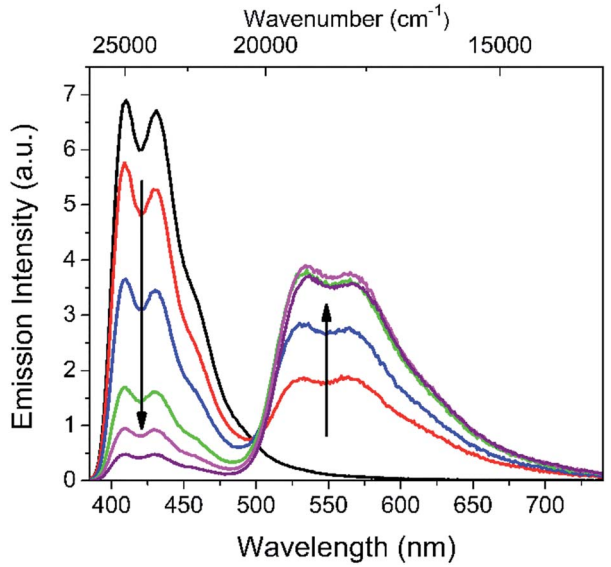

Fig. 1 Emission spectra (λ_{exc} = 375 nm) of a water dispersion of polymer micelles containing DPA (total concentration 3.5 μM) and DAE (total concentration 2 μM) at different degrees of UV-induced isomerization DAEo → DAEc (365 nm, 1.5 mW cm^{-2}). The initial spectrum (black line) was excited at 415 nm to avoid any isomerization induced by the excitation light. The intensity was subsequently scaled to represent the corresponding intensity after excitation at 375 nm.

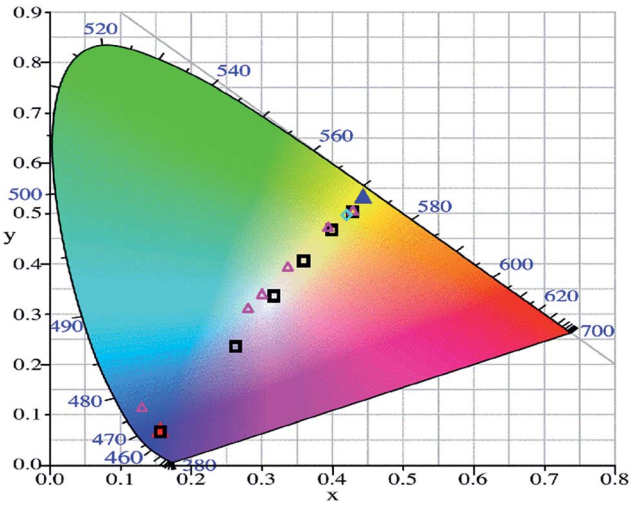

Fig. 2 CIE diagram showing the trajectories of the color changes upon UV exposure (black hollow squares) and visible light exposure (magenta hollow triangles) of the micellar cocktail containing DPA and DAE. Also shown are the coordinates for DPA alone (red solid triangle), DAEc alone (blue solid triangle), and the cocktail after a second dose of UV light, again triggering isomerization to 100% DAEc (cyan hollow square).

implies that the "dynamic range" of the color switching is close to being maximized.

Perfect white light corresponds to a CIE coordinate of (0.33, 0.33), and a common strategy of generating this type of light is to mix a blue emitter and a yellow emitter in adequate proportions. As mentioned above, this approach is "static", in the sense that each system can only generate one emission color. Our approach, however, represents a means where one and the same cocktail of **DPA** and **DAE** can be used to generate emission colors from blue to yellow, and as we hit the coordinate (0.32, 0.33) along the way, we come very close to the generation of perfect white light. It is also very encouraging to see that the blue-to-yellow emission color change is reversible, by exposure to visible light (523 nm used here) that triggers the isomerization **DAEc** → **DAEo**. This process is illustrated in the CIE diagram in Fig. 2 by the magenta hollow triangles.[38]

Exposing the cocktail to another UV dose again shifts the CIE coordinate very close to that observed for **DAEc** (cyan hollow square in Fig. 2), proving that the emission color changes are indeed due to the reversible isomerization of the **DAE** photoswitch rather than the corresponding photodecomposition.

Fig. 3 compiles the spectra of the extreme situations (the cocktail with no isomerization and complete isomerization **DAEo** → **DAEc**) as well as the reference micelles with **DPA** and **DAEc** alone, each at the same concentration as in the cocktail. From this data, it is seen that the emission intensity of **DPA** is decreased by 43% and 96% with the cocktail in 100% **DAEo** and 100% **DAEc**, respectively. Hence, it is clear that **DAEo** is quenching **DPA**. As FRET quenching is excluded, likely explanations include the formation of a non-emissive ground state complex between **DPA** and **DAEo** (static quenching) or the introduction of dynamic quenching processes, *e.g.*, photoinduced electron transfer (PET), a thermodynamically favorable process for this system (see ESI† for redox data). The results from time-resolved single photon counting (SPC) measurements are consistent with the latter, as the quenching is also reflected in the average fluorescence lifetime of **DPA**,

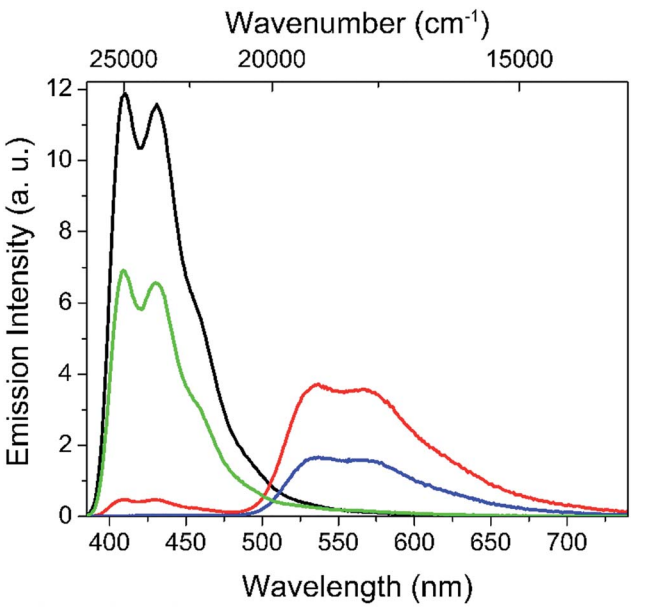

Fig. 3 Emission spectra of DPA alone (black line), DAEc alone (blue line), the cocktail DPA + DAEo (green line), and DPA + DAEc (red line), all in water dispersions of the polymer micelles. The concentration of the respective species was the same in all experiments (3.5 μM for DPA and 2 μM for DAE).

decreasing from 7.5 ns to 4.2 ns by the introduction of **DAEo**. The formation of a non-emissive ground state complex would instead have no effect on the lifetime. It is also encouraging to note that the quenching efficiency judged by the decrease in the **DPA** average lifetime, 44%, agrees very well with the corresponding result from the steady-state emission measurements, 43%.

At the other extreme, where 100% of the **DAE** population is isomerized to **DAEc**, the overall emission from this species arises from direct excitation as well as sensitization *via* FRET from the excited state of **DPA** (**DPA***). After compensation for the directly excited fraction (*cf.* blue line in Fig. 3) the FRET sensitization efficiency is estimated to 45%, that is, significantly lower than the corresponding quenching efficiency of **DPA** of 96%. Again, this discrepancy is ascribed to thermodynamically favorable PET processes originating from **DPA***, rather than the corresponding processes from **DAEc*** (see below). The results from SPC agree well with the steady-state observations, as the quenching efficiency from the time-resolved data is determined to 91% (average **DPA** lifetime decreasing from 7.5 ns to 0.7 ns by the introduction of **DAEc**), which is close to the 96% from steady-state measurements. The subsequent decay of **DAEc*** is not affected by the presence of **DPA** (average lifetime of 2.5 ns for **DAEc*** alone and 2.5 ns in the cocktail). Hence, we can exclude PET processes contributing to the overall deactivation of **DAEc***, fully consistent with the much less favorable driving force for these processes (see ESI† for a comprehensive evaluation of the SPC data and redox energies).

The variation of the overall emission intensity with increasing isomerization **DAEo** → **DAEc** is worth commenting on (see Fig. 4). Initially, the emission quantum yield is 0.57. Here, the emission is exclusively accounted for by the **DPA** fluorophore, quenched from the intrinsic quantum yield of unity by PET processes. Initial UV exposure results in a slight increase of the overall emission intensity. This is ascribed to activation of FRET sensitization, which in turn decreases the efficiency of non-radiative PET losses from **DPA***. In addition, direct excitation of **DAEc** is also contributing to the increase. The subsequent minor decrease is explained by the onset of PET from **DPA*** to **DAEc**, competing with the FRET process.

Finally, choosing the **DAE** concentration implies a trade-off between the decreased overall emission intensity resulting from non-radiative losses from PET reactions, and maximizing the dynamic range of the CIE trajectory. At 2 μM **DAE**, the resulting initial emission intensity of **DPA** in the cocktail corresponds to a quantum yield of 0.57. We find this satisfactory, as it both allows for coverage of all emission colors between pure **DPA** and **DAEc**, as well as maintaining a relatively constant overall emission intensity irrespective of the degree of **DAE** isomerization.

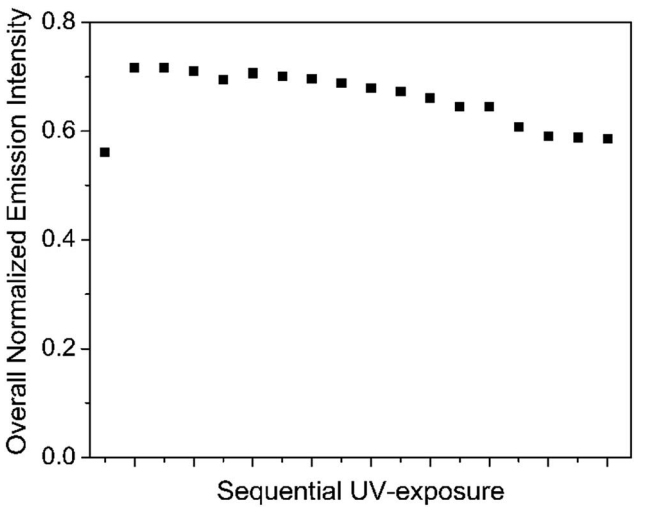

Fig. 4 Variations of the overall emission intensity with increasing UV-induced isomerization **DAEo** → **DAEc** in the micellar cocktail. All emission spectra were converted to a wavenumber scale and intensity-corrected (I(wavenumber) = $I(\lambda)\lambda^2$) before integration was performed.

Conclusions

We have presented a FRET-based self-assembled construct where the emission color is reversibly controlled by means of photonic stimuli. As the system exhibits the CIE coordinates (0.32, 0.33), we achieve virtually perfect white-light generation. Due to the strongly emissive nature of the photochromic acceptor, the resulting fluorescence output remains high throughout operation within the whole range of emission color.

Acknowledgements

This work was financed by the Swedish Research Council VR (grant 622-2010-280, JA), the National Science Foundation (CHE-1049860, FMR), and the Spanish Ministry of Economy and Competitiveness (MINECO Project CTQ2015-65439-R, JH and GG).

References

1 C. H. Li and S. Y. Liu, *Chem. Commun.*, 2012, **48**, 3262–3278.
2 S. Mukherjee and P. Thilagar, *Dyes Pigm.*, 2014, **110**, 2–27.
3 V. K. Praveen, C. Ranjith and N. Armaroli, *Angew. Chem., Int. Ed.*, 2014, **53**, 365–368.
4 Z. M. Hudson, D. J. Lunn, M. A. Winnik and I. Manners, *Nat. Commun.*, 2014, **5**, 3372.
5 K. Jiang, S. Sun, L. Zhang, Y. Lu, A. G. Wu, C. Z. Cai and H. W. Lin, *Angew. Chem., Int. Ed.*, 2015, **54**, 5360–5363.
6 J. H. Kim, B. K. An, S. J. Yoon, S. K. Park, J. E. Kwon, C. K. Lim and S. Y. Park, *Adv. Funct. Mater.*, 2014, **24**, 2746–2753.
7 J. E. Kwon, S. Park and S. Y. Park, *J. Am. Chem. Soc.*, 2013, **135**, 11239–11246.
8 R. Wang, J. Peng, F. Qui, Y. L. Yang and Z. Y. Xie, *Chem. Commun.*, 2009, 6723–6725.
9 J. Chen, P. S. Zhang, G. Fang, P. G. Yi, F. Zeng and S. Z. Wu, *J. Phys. Chem. B*, 2012, **116**, 4354–4362.
10 H. B. Cheng, H. Y. Zhang and Y. Liu, *J. Am. Chem. Soc.*, 2013, **135**, 10190–10193.
11 P. Coppo, M. Duati, V. N. Kozhevnikov, J. W. Hofstraat and L. De Cola, *Angew. Chem., Int. Ed.*, 2005, **44**, 1806–1810.

12 S. A. Díaz, L. Giordano, T. M. Jovin and E. A. Jares-Erijman, *Nano Lett.*, 2012, **12**, 3537–3544.
13 H. T. Feng, J. B. Xiong, Y. S. Zheng, B. A. Pan, C. Zhang, L. Wang and Y. S. Xie, *Chem. Mater.*, 2015, **27**, 7812–7819.
14 B. P. Jiang, D. S. Guo, Y. C. Liu, K. P. Wang and Y. Liu, *ACS Nano*, 2014, **8**, 1609–1618.
15 J. Karpiuk, E. Karolak and J. Nowacki, *Phys. Chem. Chem. Phys.*, 2010, **12**, 8804–8809.
16 H. J. Kim, D. R. Whang, J. Gierschner, C. H. Lee and S. Y. Park, *Angew. Chem., Int. Ed.*, 2015, **54**, 4330–4333.
17 S. Kim, S. J. Yoon and S. Y. Park, *J. Am. Chem. Soc.*, 2012, **134**, 12091–12097.
18 C. H. Li, Y. X. Zhang, J. M. Hu, J. J. Cheng and S. Y. Liu, *Angew. Chem., Int. Ed.*, 2010, **49**, 5120–5124.
19 M. Montalti, G. Battistelli, A. Cantelli and D. Genovese, *Chem. Commun.*, 2014, **50**, 5326–5329.
20 A. Nano, M. P. Gullo, B. Ventura, N. Armaroli, A. Barbieri and R. Ziessel, *Chem. Commun.*, 2015, **51**, 3351–3354.
21 S. Park, J. E. Kwon, S. H. Kim, J. Seo, K. Chung, S. Y. Park, D. J. Jang, B. M. Medina, J. Gierschner and S. Y. Park, *J. Am. Chem. Soc.*, 2009, **131**, 14043–14049.
22 Q. K. Qi, J. Y. Qian, S. Q. Ma, B. Xu, S. X. A. Zhang and W. J. Tian, *Chem.–Eur. J.*, 2015, **21**, 1149–1155.
23 K. S. Sanju, P. P. Neelakandan and D. Ramaiah, *Chem. Commun.*, 2011, **47**, 1288–1290.
24 Y. Shiraishi, C. Ichimura, S. Sumiya and T. Hirai, *Chem.–Eur. J.*, 2011, **17**, 8324–8332.
25 Y. J. Yang, M. Lowry, C. M. Schowalter, S. O. Fakayode, J. O. Escobedo, X. Y. Xu, H. T. Zhang, T. J. Jensen, F. R. Fronczek, I. M. Warner and R. M. Strongin, *J. Am. Chem. Soc.*, 2006, **128**, 14081–14092.
26 Z. Y. Zhang, Y. S. Wu, K. C. Tang, C. L. Chen, J. W. Ho, J. H. Su, H. Tian and P. T. Chou, *J. Am. Chem. Soc.*, 2015, **137**, 8509–8520.
27 L. L. Zhu, X. Li, Q. Zhang, X. Ma, M. H. Li, H. C. Zhang, Z. Luo, H. Ågren and Y. L. Zhao, *J. Am. Chem. Soc.*, 2013, **135**, 5175–5182.
28 L. Y. Zhu, W. W. Wu, M. Q. Zhu, J. J. Han, J. K. Hurst and A. D. Q. Li, *J. Am. Chem. Soc.*, 2007, **129**, 3524–3526.
29 C. F. Chamberlayne, E. A. Lepekhina, B. D. Saar, K. A. Peth, J. T. Walk and E. J. Harbron, *Langmuir*, 2014, **30**, 14658–14669.
30 D. V. Kozlow and F. N. Castellano, *J. Phys. Chem. A*, 2004, **108**, 10619–10622.
31 D. Gust, J. Andréasson, U. Pischel, T. A. Moore and A. L. Moore, *Chem. Commun.*, 2012, **48**, 1947–1957.
32 K. Uno, H. Niikura, M. Morimoto, Y. Ishibashi, H. Miyasaka and M. Irie, *J. Am. Chem. Soc.*, 2011, **133**, 13558–13564.
33 Embedded in hydrophobic nanoparticles, the fluorescence quantum yield of photochromic molecules (*e.g.*, spiropyran derivatives) may experience an increase up to *ca.* 0.2. See for example ref. 28.
34 I. Yildiz, S. Impellizzeri, E. Deniz, B. McCaughan, J. F. Callan and F. M. Raymo, *J. Am. Chem. Soc.*, 2011, **133**, 871–879.
35 E. Rampazzo, S. Bonacchi, R. Juris, M. Montalti, D. Genovese, N. Zaccheroni, L. Prodi, D. C. Rambaldi, A. Zattoni and P. Reschiglian, *J. Phys. Chem. B*, 2010, **114**, 14605–14613.
36 D. Genovese, S. Bonacchi, R. Juris, M. Montalti, L. Prodi, E. Rampazzo and N. Zaccheroni, *Angew. Chem., Int. Ed.*, 2013, **52**, 5965–5968.
37 The concentrations of **DPA** and **DAE** are significantly higher in the micelles compared to the apparent "bulk concentration" estimated from UV/vis absorption measurements. With a 1.35 μM concentration of the micelles in solution (see ESI†), and the assumption that the diameter of the micellar hydrophobic core is 10 nm (*cf.* the hydrodynamic diameter of 15 nm), the intra-micellar concentrations of **DPA** and **DAE** are *ca.* 8 mM and 5 mM, respectively. This results in intermolecular donor–acceptor distances that allow for FRET reactions to occur with high efficiency. It should be stressed that there are no signs of self-quenching of the respective fluorophore in the micelles, despite the high effective concentrations. This is apparent from the steady-state intensities of the monomers, which scale linearly with the micellar concentrations of **DPA** and **DAEc** (see ESI† for details). Moreover, the fluorescence quantum yields of **DPA** and **DAEc** are not significantly changed in the micelles compared to the corresponding numbers in acetonitrile at μM concentrations. We ascribe the absence of self-quenching to the limited diffusion of the fluorophores embedded in the decylside chains inside the micelles.
38 The observed "hysteresis" is due to an increase of the weak emission from **DAEo** with time (maximum at around 500 nm). The reason for this increase is still unclear.